

EXPERIMENTAL STUDY ON FIRE RESISTANCE OF SQUARE HOLLOW SECTION (SHS) TUBULAR T-JOINT UNDER AXIAL COMPRESSION

J. Yang¹, Y.B. Shao^{2,*} and C. Chen¹

¹Graduate student, School of Civil Engineering, Yantai University, PR China

²Professor, School of Civil Engineering, Yantai University, PR China

*(Corresponding author: E-mail: cybshao@ytu.edu.cn)

Received: 8 November 2012; Revised: 1 January 2013; Accepted: 3 January 2013

ABSTRACT: The main purpose of this paper is to study the fire resistance and failure mode of the square hollow section (SHS) T-joint at elevated temperatures under axial compression. Experimental tests on two full-scale square tubular T-joints with different geometries are carried out. The specimens are set to sustain constant compressive loading at brace end during the heating process. The environmental temperature around the specimens is in accordance with ISO 834 heating curve. The temperature on the tube surface and the deforming process of the two T-joints are both measured till the failure of the specimens. The experimental results show that the failure process of both specimens includes three stages. The final failure mode of both specimens is local buckling on the chord surface near the brace/chord intersection while there is no clear global deformation on the T-joint surfaces. In comparison, the T-joint specimen with smaller brace-to-chord diameter ratio has a more gradual and longer time of deforming process before final failure, which shows the geometry of the tubular joint has an effect on the failure mechanism.

Keywords: SHS tubular T-joint, fire resistance, experimental study, axial compression, failure mode

1. INTRODUCTION

Tubular structures can be found easily in industry buildings, long-span bridges, railway stations and towers for their characteristics of light weight, high strength and easy fabrication. In these structures, tubular joints are the critical parts due to high stress concentration at the weld toe caused by discontinuous stiffness and residual stress produced by welding process. A typical tubular joint is consisted of a chord member and several brace members. For hollow section joints, failure often occurs on the chord surface near the brace/chord intersection as the radial stiffness of the chord is much weaker than the axial stiffness of the brace. In addition, the material properties of steel are quite sensitive to high temperature. In general, the elastic modulus and the yield stress of steel both reduce extremely at an elevated temperature which makes the joints fail easier. Therefore, it is considerably important and necessary to study the mechanical behavior of tubular joints under fire condition.

Considerable work has been carried out on the fire resistance of beams, columns and beam-column joints in building structures [1-9]. However, there is relatively less research work on tubular joints. For tubular T-joints, the mechanical behavior under various loading conditions at room temperature has been studied experimentally and numerically in the literature, and such work can be found in Refs [10-14]. Studies on mechanical performance of tubular joints under fire condition mostly focus on the phases of loading at constant-high temperature and post-fire loading to failure. Among these studies, Liu et al. [15-16] studied the ultimate bearing capacity of circular tubular T-joints with and without stiffened rings at elevated temperatures using finite element method. It was found that the bearing capacity of the joint decreased as the temperature increased and that the static strength has been improved obviously after reinforcing the joint with several rings. In addition, the number of reinforced ring in design is recommended to be 1 or 3. Nguyen et al. [17-18] carried out both experimental and parametric studies on the static strength of several CHS T-joints subjected to

brace axial compression at different elevated temperatures. It was found that the ultimate bearing capacity of the joint decreased obviously as the temperature increased and parameters β and γ have more significant effects on the static strength of the joints. An experimental and parametric study on the post-fire behavior of circular hollow section T-joints was conducted by Jin et al [19]. Residual strengths of the joints after fire exposure and the influence of geometric parameters were studied. The results indicated that the failure of the joints is due to local buckling of the chord member near the brace/chord intersection, and parameter β has more significant effect on load-bearing capacity of the T-joint than γ when the joint endures same elevated temperature. Very scarce research work on tubular joints under heating state of fire has been conducted in recent years. Yu et al. [20] carried out an experimental investigation to study the mechanical behavior of an impacted steel tubular T-joint under fire condition. The joint specimen was impacted first and then heated up under constant loading. The experimental results showed that local buckling failure occurred on the chord wall and that the critical temperature of the impacted joint is higher than the one without impact loading. However, all above research work is only focused on circular tubular T-joints and there is considerably less research work on fire resistance of square hollow section T-joints. Thus, it is necessary to conduct further investigation on the mechanical behavior of SHS tubular joints under fire condition. This study is thus carried out to analyze the fire resistance of SHS tubular joints through experimental tests.

2. EXPERIMENTAL TEST ARRANGEMENTS

2.1 Test Specimens

Two square hollow section T-joints named SP-T₁ and SP-T₂ respectively are tested. Figure 1 shows the appearance of a T-joint specimen. The brace member is directly welded onto the upper surface of the chord member by using penetration weld, and the brace is profiled around the intersection before welding to ensure the welding quality. For convenience to apply axial load at brace end, an end plate, 300mm×300mm×20mm (length by width by thickness), is welded on the brace end. Two end plates with four bolt holes, 450mm×400mm×20mm (length by width by thickness), are welded on two chord ends to connect the specimen to supports. Figure 2 shows the schematic view and definitions of some symbols for T-joint specimen. The geometric dimensions of the specimens are listed in Table 1. As is shown in Table 1, the two T-joints have same geometrical dimensionless parameters except for the ratio of brace diameter to chord diameter of the specimen, β . The values of this parameter are 0.4 and 0.8 for the two specimens respectively. This design is then to investigate the effect of parameter β on fire performance of the T-joints directly through experimental results. In addition, the outer length (b_0) of the two specimens is constant which means the heating height of the braces in furnace is equivalent. As the critical part of the joint is the area near the brace/chord intersection, the two T-joint specimens are heated locally around this region. The heating lengths of brace and chord in electric heating furnace are 400mm and 895mm respectively. All the square steel tubes and end plates are fabricated with Q235B steel which is commonly used in Chinese construction industry. The tensile coupon specimens are designed and tested according to China code of metallic material--tensile testing at ambient temperature (GBT 228-2002). The tensile test rig is shown in Figure 3. The measured steel material properties are listed in Table 2, and they are the fundamentals in future numerical study. In Table 2, the yield stress and the ultimate tensile stress are defined as f_y and f_u respectively, and E denotes the elastic modulus.



Figure 1. Appearance of a T-joint Specimen

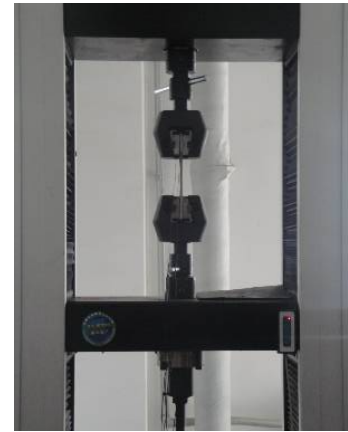


Figure 3. Material Tensile Test Rig

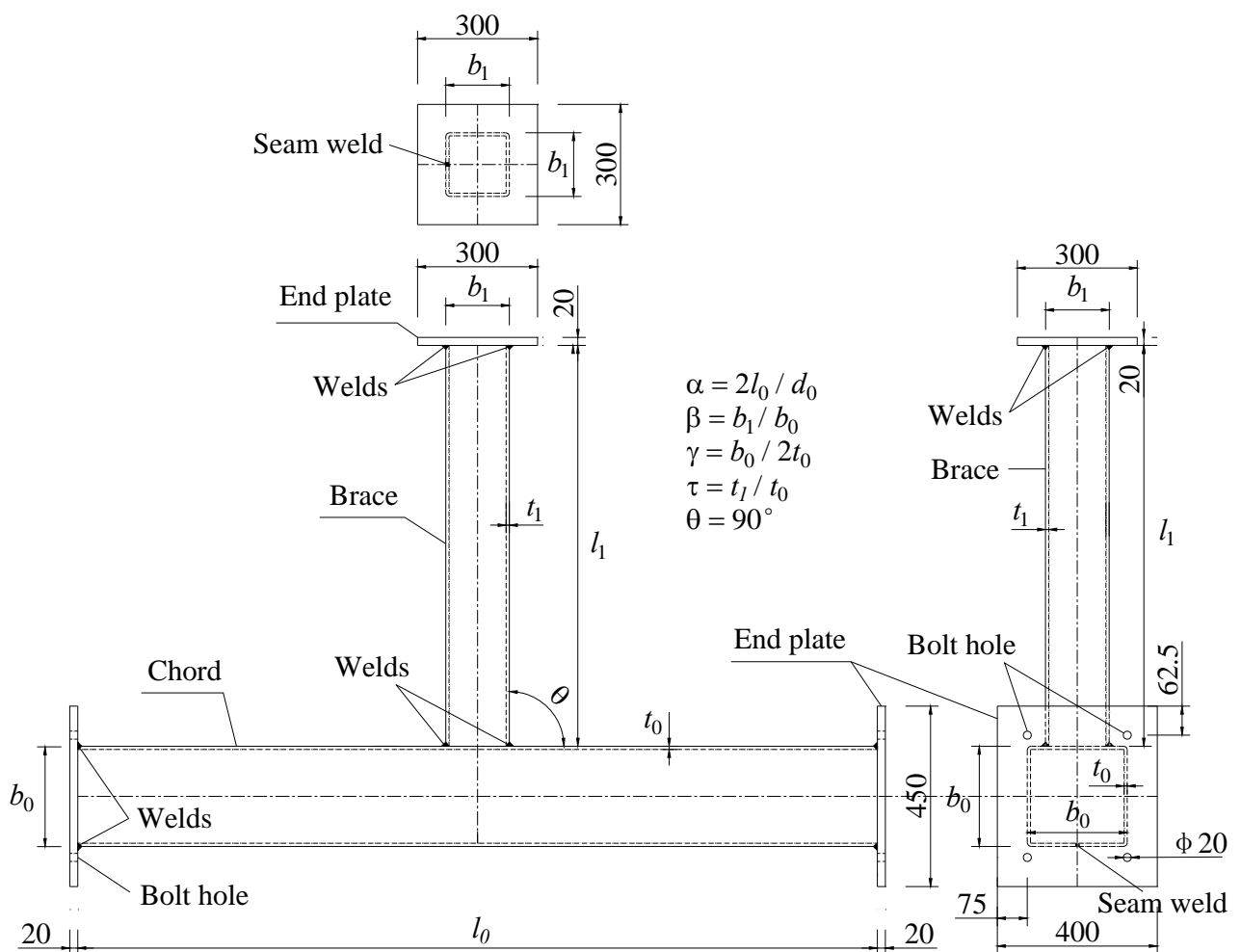


Figure 2. Schematic View and Definition of Symbols for T-joint Specimen

Table 1. Geometrical Dimensions of T-joint Specimens

| Specimen | b_0 (mm) | b_1 (mm) | t_0 (mm) | t_1 (mm) | l_0 (mm) | l_1 (mm) | α | β | γ | τ |
|-------------------|------------|------------|------------|------------|------------|------------|----------|---------|----------|--------|
| SP-T ₁ | 200 | 80 | 5 | 5 | 2000 | 1000 | 20 | 0.4 | 20 | 1.0 |
| SP-T ₂ | 200 | 160 | 5 | 5 | 2000 | 1000 | 20 | 0.8 | 20 | 1.0 |

Table 2. Results of Material Tensile Tests

| Tube diameter (mm) | f_y (MPa) | f_u (MPa) | E (MPa) |
|--------------------|-------------|-------------|-----------|
| 80 | 399.5 | 463.9 | 187432 |
| 160 | 364.5 | 518.8 | 183834 |
| 200 | 320.7 | 442.8 | 202607 |

2.2 Test Rig

The experimental tests of T-joints are carried out in a specially designed electric heating furnace. To heat specimens uniformly, the resistance coils, which are placed on the inner wall of the furnace and are used to produce heat when electric current is flowing in them, are arranged evenly in the furnace. The air temperature in a space of 900mm×600mm×700mm (length by width by height) can be heated up to 1200 °C. Compared with gas/oil furnace, electric heating furnace has several advantages. Firstly, the air temperature in heating process can be controlled accurately by 1 °C. Secondly, the test cost is much lower. During the experimental tests, the air temperatures near the surfaces of square tubular T-joint is necessary to agree with ISO 834 standard heating curve. Before experiments, the furnace is tested several times, and the final temperature versus time curve obtained from testing is compared with ISO 834 standard heating curve, and the comparison is shown in Figure 4. As shown in Figure 4, the air temperatures around T-joint surfaces in furnace agree with the standard curve reasonably well except for the beginning stage. However, the temperatures near resistance coils are higher than air temperatures. In order to satisfy the standard fire condition, convection and radiation should be taken into consideration separately for electric heating furnace. In future finite element modelling, the air temperature in furnace will be used for convection and the resistance coils temperature will be used for radiation.

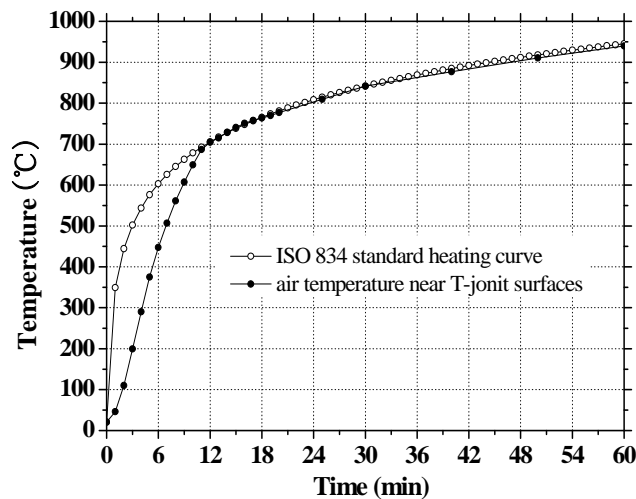


Figure 4. Comparison of Temperature Versus Time Curves

Besides electric heating furnace, the test rig includes support and loading devices. The whole test rig is shown in Figure 5. Each support is consisted of two I-section beams, two end plates and several slats. The end plates of the chord are connected to the support by four bolts. Actually, the support can not supply enough stiffness to constrain axial expansion and rotation of chord during the heating process. Therefore, the boundary condition can not be regarded as fixed constraint in finite element modelling. The main part of the loading device is a jack. The maximum compressive force provided by the jack is 300 kN. Before heating the square tubular T-joint, an axial compressive load is applied by the jack at the brace end while the freedoms in other directions of brace end are free.

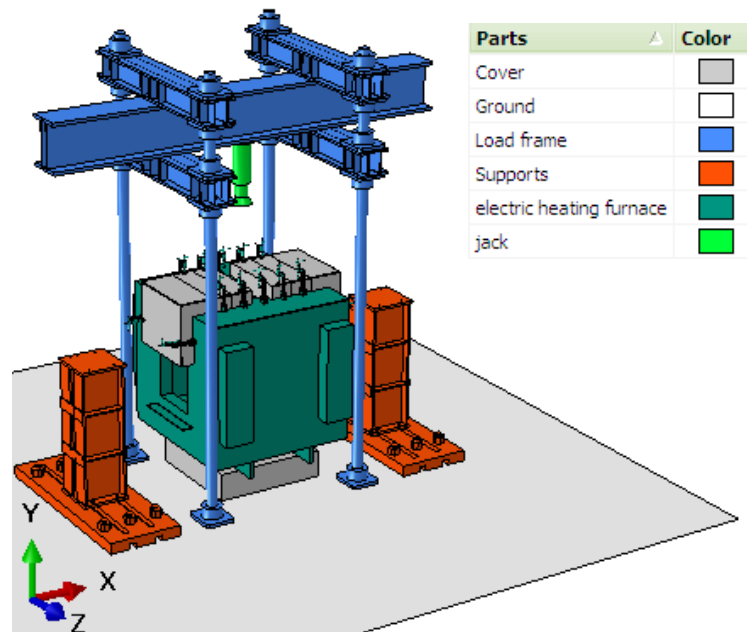


Figure 5. 3D View of Test Devices

2.3 Measuring Method and Instruments

For each SHS T-joint specimen, the displacements at three points are measured during the tests including two on chord and one at brace end. The positions of the two points on the chord are shown in Figure 6. The brace end displacement is measured by LVDT directly while the displacements of points Dc-1 and Dc-2 can not be measured directly because of the high temperature in furnace. Therefore, an indirect method to obtain the displacement is adopted by using two fixed pulleys and a piece of molybdenum wire. The schematic is shown in Figure 7. One end of the wire is fixed on the iron rod which is welded at the measure point and the other end of the wire is connected with a LVDT. The two pulleys are used to arrange the LVDT conveniently by changing the direction of the molybdenum wire. A weight of 250g is tied at the end of LVDT to keep molybdenum straight during the experimental tests. The axial applied load is measured by force sensor which is connected with a computer. As shown in Figure 8, the temperatures at three points on each T-joint specimen are tested by using K-type nickle-chromium thermocouples. The measure point on brace wall is 200 mm away from the chord upper surface. In addition, the temperatures of air and resistance coils are also measured during the tests. All the temperatures can be shown on screen of control box of the heating furnace. The control box is shown in Figure 9.

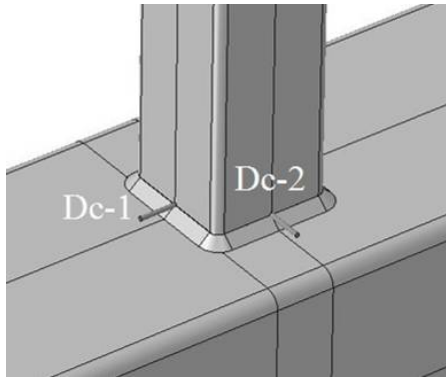


Figure 6. Arrangement of Displacement Measure Points

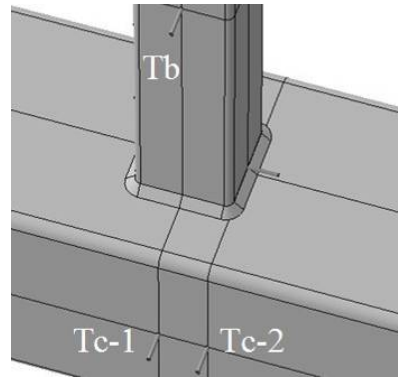


Figure 8. Arrangement of Temperature Measure Points

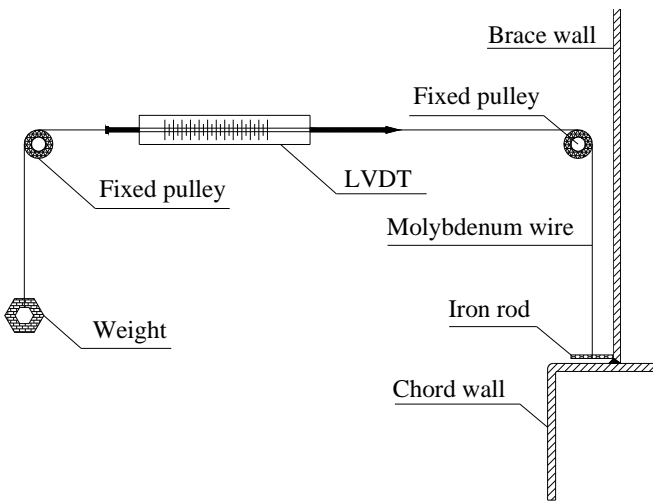


Figure 7. Schematic of Indirect Measure Method



Figure 9. View of Control Box of Heating Furnace

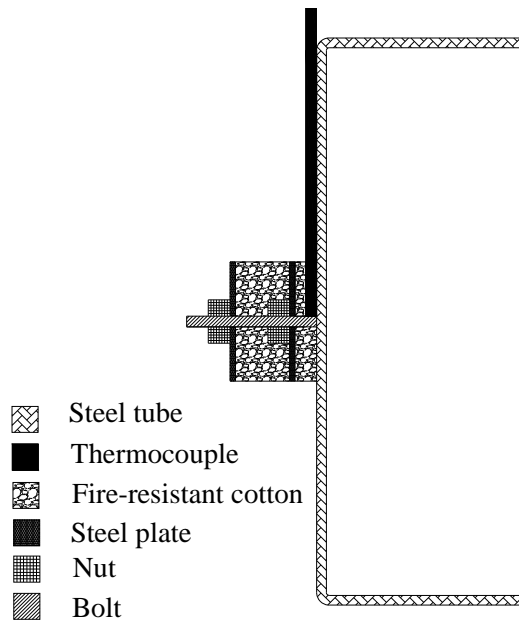


Figure 10. View of the Fixed Thermocouple

To measure tube surface temperature accurately, thermocouple should not expose to air and be affected by temperature of air in the furnace. Hence, the end of the thermocouple should be packed with fire-resistant cotton which is shown in Figure 10. Before fixing thermocouple, a bolt is welded on the measure point. A thermocouple is firstly placed near the bolt and covered by a layer of fire-resistant cotton. A thin steel plate and a nut are then used to fix thermocouple. Afterwards, the above two steps are repeated to ensure the thickness of the cotton.

2.4 Test Procedure

Figure 11 shows a specimen in heating furnace. The fire resistance tests of SHS T-joint specimens include two main steps: loading stage and heating stage. Before heating the joint, a constant axial load was applied at the brace end. The axial load ratio n is about 0.5, which means the pre-load is half of the ultimate bearing capacity of corresponding SHS T-joint at ambient temperature. The ultimate strengths of SP-T₁ and SP-T₂ obtained from finite element analyses by using ABAQUS are 46kN and 154kN respectively. The static strengths are determined by deformation limit provided by Zhao [21]. The pre-loads at brace end are then determined to be 23kN and 77kN respectively. The finite element models are built using solid elements to generate the meshes of the two joints. Geometrical and material nonlinearity are both taken into consideration in the models. The mechanical properties of steel material can be found in Table 2, and the stress-strain relationship is defined as ideal elastic-plastic model. As it is very mature for calculating the ultimate strength of tubular joints by using finite element method, this technique is not described in details in this study. The pre-load is kept for several minutes before heating stage to ensure the specimen is in a stable state. Thereafter, the SHS T-joint is heated locally according to a predefined heating curve. During the heating process, the temperatures of the air in the furnace and of the heating wires are plotted together as shown in Figure 12. It can be seen that the temperature of the air is lower because there is a heat transfer process between the air and the heating wires. However, the temperature increase is regular for both the air and the heating wires.



Figure 11. View of a Specimen in Heating Furnace

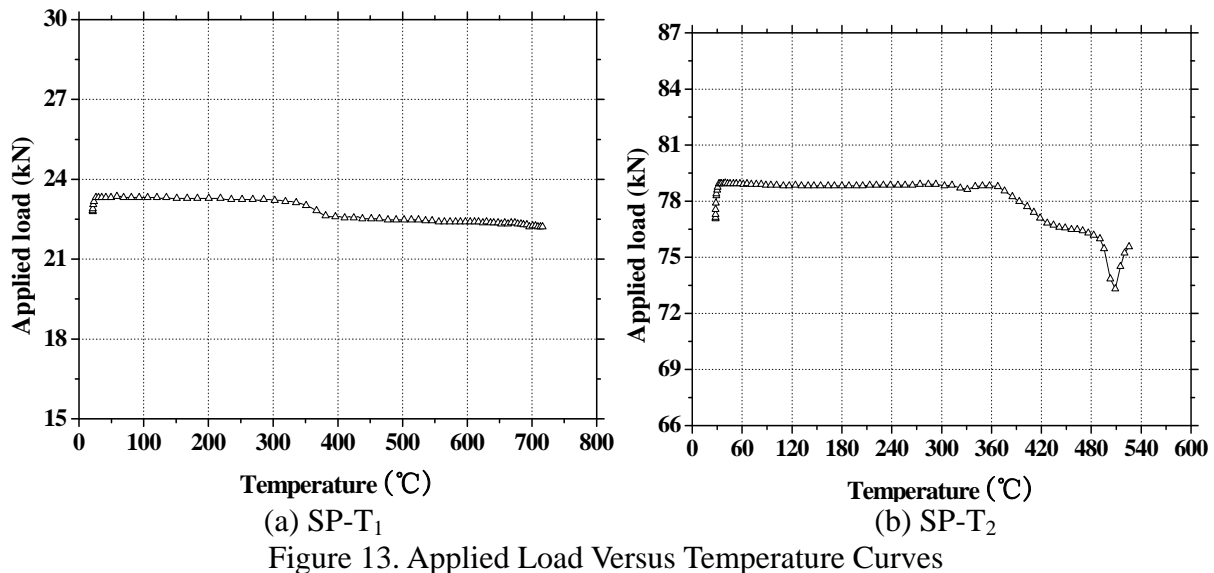
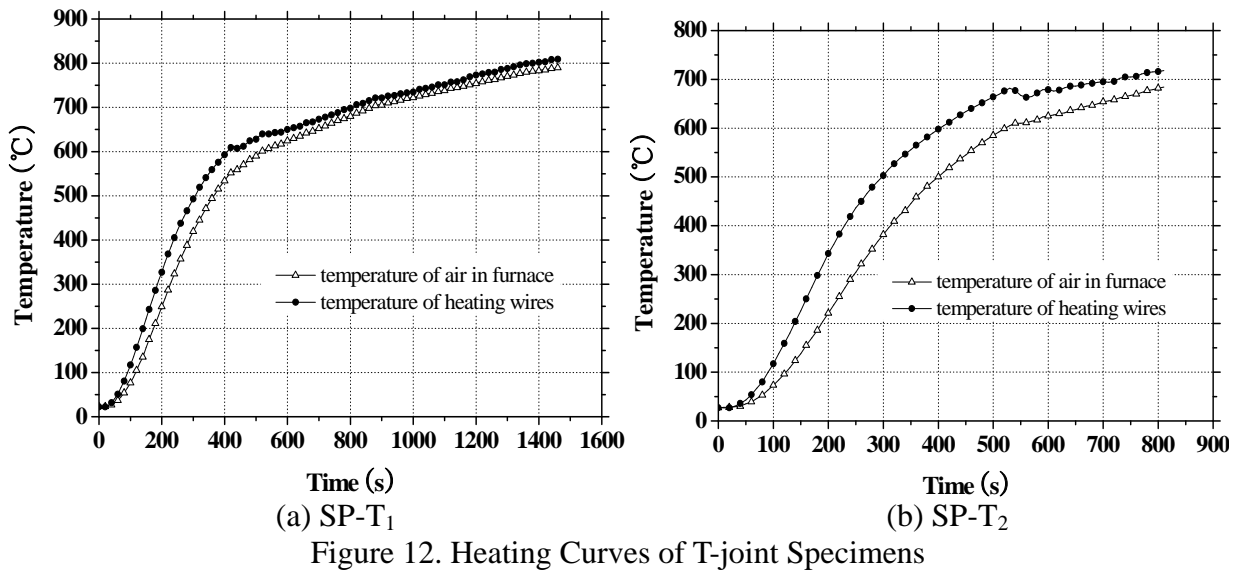


Figure 13 shows the actual applied load versus chord average temperature curve. The applied load is steady in most heating time. However, there is also smaller change of the loading value during the experimental tests. The reason is that the hydraulic device is not sensitive to tiny changes of pressure, and hence it can not react unless the change value of load is big or small enough. In addition, as the brace end is not constrained, the brace can move up firstly due to expansion of steel and then move down due to the compressive displacement of the chord surface.

3. RESULTS AND ANALYSES

3.1 Failure Mode

In general, local buckling failure of chord is observed for both specimens SP-T₁ and SP-T₂, which is shown in Figure 14. The main reason is that the transverse stiffness of chord is much lower than the axial stiffness of brace when the specimen is subjected to axial external load at brace end. For the first specimen SP-T₁, there is no obvious deformation on the brace wall. Additionally, the bottom surface of the chord has clear bulge deformation. The reason may be that residual deformation caused by welding exists. In this case, the bottom surface of the chord is not flat, and

such deformation may occur if the bottom surface has an initial convex deflection. Hence, initial deformation should be taken into consideration in future finite element modelling. For the second specimen SP-T₂, minor deformation occurred on the brace wall near the weld toe while there is no clear deformation on the bottom surface of the chord.

As the elastic modulus is deteriorated severely at elevated temperature, the flexural stiffness of the top surface of the chord reduces greatly. The existence of high stress concentration around the weld on the chord surface causes failure to occur in local region near the weld toe. In high temperature, such failure is especially easier because the deterioration of the flexural stiffness of top surface of the chord. Figure 14 shows local failure around the weld toe is much dominant for the T-joints at elevated temperature. The chord, however, has very minor global flexural deformation during the heating process.

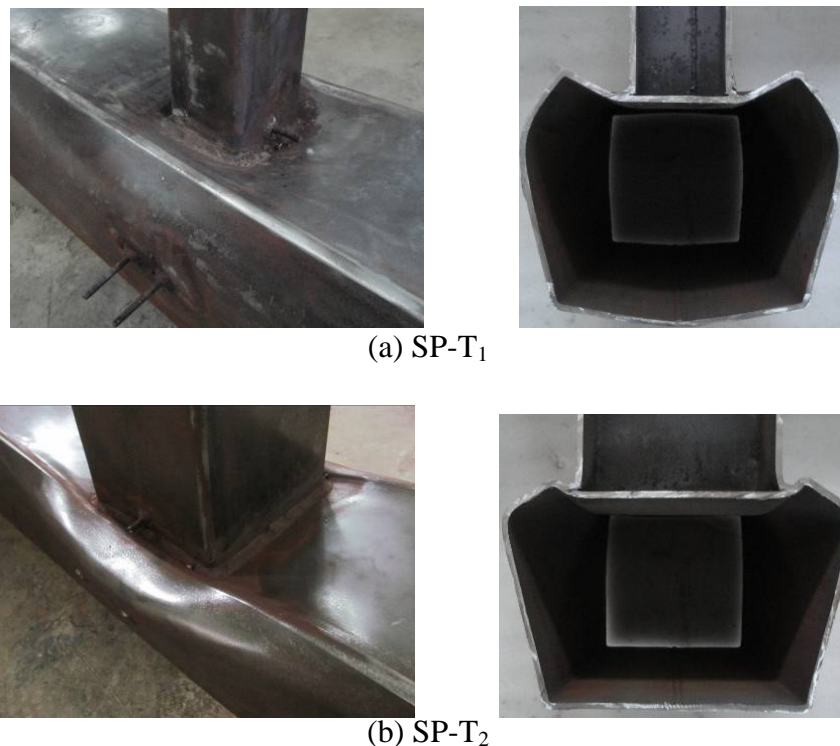


Figure 14. Failure Mode of the Specimens

3.2 Displacement Versus Temperature Curves

To reduce measurement error caused by expansion of molybdenum wire during heating the T-joint, the elongation of a molybdenum wire with a 250 g weight in fire condition is tested before the experimental tests. The heated length of the wire is 900 mm. The results obtained from testing are shown in Figure 15. It is clear that a total displacement of approximate 1.7mm occurs in the molybdenum wire. This displacement should be extracted from the total displacement of the specimen.

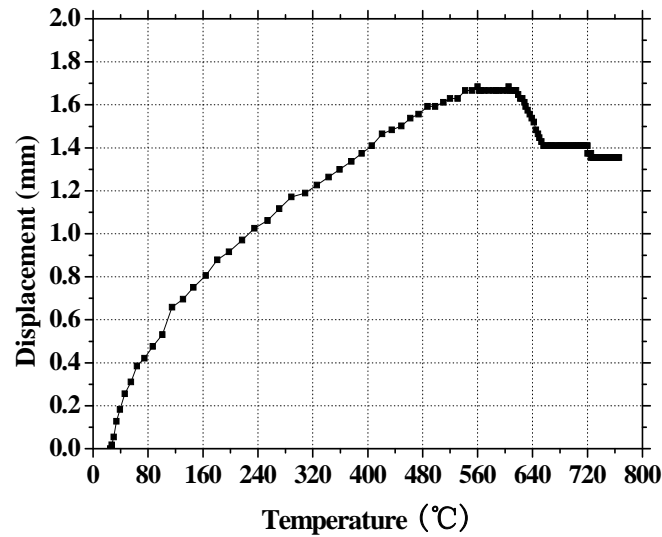


Figure 15. Displacement Versus Temperature Curve of Molybdenum Wire

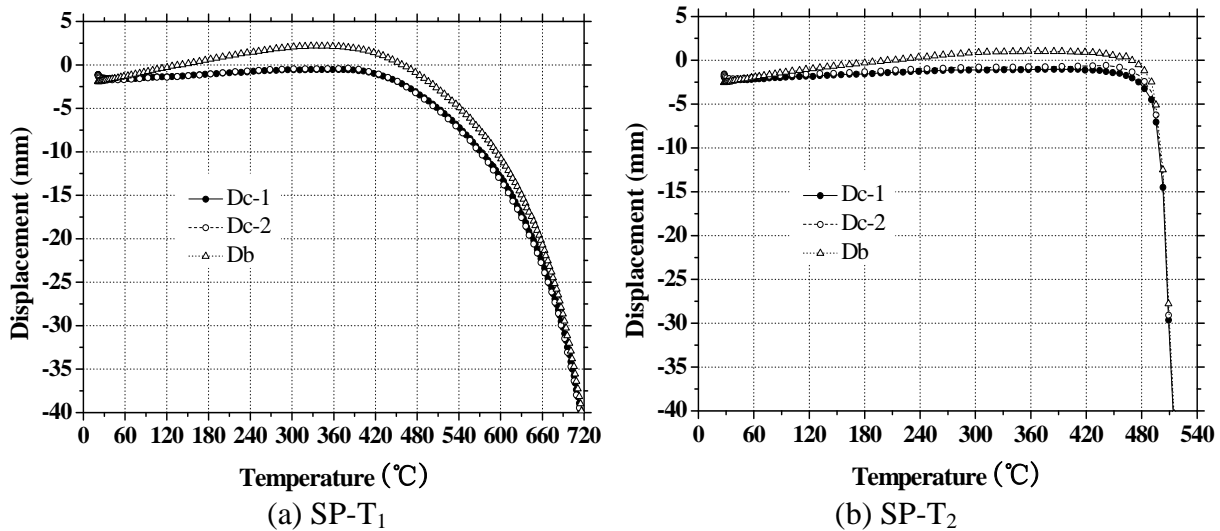


Figure 16. Corrected Displacement Versus Temperature Curves of T-joint Specimens

After eliminating the influence of the molybdenum wire, the curves of displacement versus temperature for both specimens obtained from experimental tests are plotted in Figure 16. A negative displacement denotes a compressive deformation. It can be seen from the curves that there are three stages in failure process of T-joint specimen in fire condition. In the first stage, the initial displacement caused by pre-load decreases slightly as the temperature increases. In this stage, expansion of the specimen in heating process is dominant, and such expansion will definitely reduce the compressive deformation. As the brace end is not fixed in its axial direction, the brace has a tensile deformation due to expansion, which can reduce the compressive displacement of the brace. It can also be seen that the decrease of the compressive displacement of the brace has an approximately linear relationship with the increase of the temperature in this stage.

In the second stage, the displacements begin to increase gradually after the temperature exceeds certain value. In this stage, the expansion of the steel can not compensate for the deterioration of the steel stiffness and steel strength, and hence expansion is not still dominant. The deterioration of steel mechanical properties becomes a key factor to cause the specimens to deform gradually. In the last stage, the displacements increase abruptly and drastically which means the failure of T-joint specimens.

However, there are some differences between the two specimens. For the first specimen, it can be seen that a larger expansion displacement occurs in the first stage. Additionally, the failure process of the first specimen seems to be more gradual. Figure 16(b) shows the displacement of the second specimen increases suddenly in a much faster way after temperature exceeds 500°C. This means the failure occurs in a much shorter time for SP-T₂. Further study is necessary to be conducted for studying the effect of joint geometry on the failure mode.

3.3 Displacement Versus Time Curves

The displacement versus time curves for specimen SP-T₁ and SP-T₂ obtained from experimental tests are plotted in Figure 17. As shown in Figure 17, the curves can also be divided into three stages. In the first stage (time less than 200 seconds), the displacement is almost unchanged because the material property of the steel in this time has minor change. In the second stage (200 seconds ~ 600 seconds for the first specimen, and 200 seconds ~ 700 seconds for the second specimen), a positive displacement occurs and its value increases with the increase of temperature. This positive displacement is due to the expansion of the chord tube in transverse direction in higher temperature. In the third stage (after 600 seconds for the first specimen, and after 700 seconds for the second specimen), the compressive displacement for both specimens increases. However, the displacement of the first specimen increases quite gradually while it increases sharply for the second specimen. It can be seen from Figure 17(b) that the displacement increases to 40 mm in the third stage within 100 seconds for the second specimen. For the first specimen, however, such time increases to be more than 800 seconds, which means the deformation of this specimen has an accumulating process.

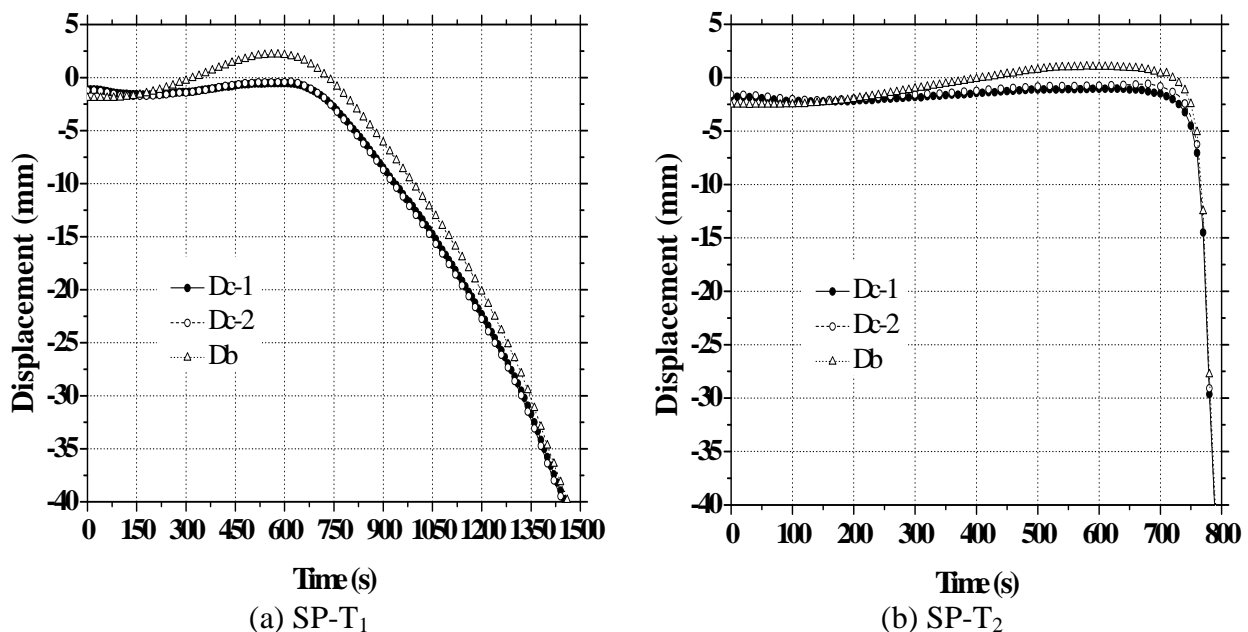


Figure 17. Displacement Versus Time Curves of T-joint Specimens

The relationship between the displacement and the heating time can be explained from Figure 14. As seen from the final failure mode of the specimens after heating process, most deformation is caused by the top surface of the chord around the brace/chord intersection. From the view of the cross section of the specimens after tests, the top surface of the chord can be simplified to be a plate supported by the two side walls of the chord tube. The top surface of the chord inside the brace tube can not deform due to the constraints of the brace member. The remaining top surface of the chord, however, has a bending deformation when the joint is subjected to compressive loading at brace end. For the first specimen, the value of β is smaller than that of the second specimen, which means

a larger region of the top surface of the chord behaves as a bending plate, as shown in Figure 14(a). The two side walls of the chord tube provide elastic support for the top surface, and they deform cooperatively. As the bending deformation of the top surface of the chord is an accumulating process, the displacement increases gradually. However, for the second specimen, as seen from Figure 14(b), a much bigger value of β causes most top surface of the chord to be inside the brace tube. Therefore, the deformation of the top surface is restricted by the brace. There is much minor bending deformation of the top surface of the chord. The two side walls of the chord tube can be still considered as supports to the top surface although the top surface can not bend easily. When the temperature increases to certain value, the deterioration of the steel material causes the stiffness of the tube wall to reduce greatly, and the two side walls of the chord fail suddenly. This is why the displacement of the second specimen increases sharply after the heating time exceeds certain value.

4. CONCLUSIONS

Experimental study for fire resistance of square hollow section T-joints has been provided in this paper. The failure process and the failure mode for the tested specimens have been studied. From experimental observation, it is found that local buckling failure occurred on the chord surface near the brace/chord intersection for both specimens. The failure process of the joints includes initial expansion of the steel material, a deforming process caused by severe deterioration of the steel materials and a quick failure of the specimen after temperature exceeds certain value. However, the geometry of the tubular joint has a remarkable effect on the failure process.

REFERENCES

- [1] Tan, Q.H., Han, L.H. and Yu, H.X., "Fire Performance of Concrete Filled Steel Tubular (CFST) Column to RC Beam Joints", *Fire Safety Journal*, 2012, Vol. 51, pp. 68-84.
- [2] Chen, J. and Young, B., "Design of High Strength Steel Columns at Elevated Temperatures", *Journal of Constructional Steel Research*, 2008, Vol. 64, pp. 689-703.
- [3] Ding, J. and Wang, Y.C., "Experimental Study of Structural Fire Behavior of Steel Beam to Concrete Filled Tubular Column Assemblies with Different Types of Joints", *Engineering Structures*, 2007, Vol. 29, pp. 3458-3502.
- [4] Qian, Z.H., Tan, K.H. and Burgess, I.W., "Numerical and Analytical Investigations of Steel Beam-to-column Joints at Elevated Temperatures", *Journal of Constructional Steel Research*, 2009, Vol. 65, No. 5, pp. 1043-1054.
- [5] Han, L.H. and Xu, L., "Tests on the Fire Resistance Concrete Filled Steel Square Tubular Columns with Protections", *China Civil Engineering Journal*, 2000, Vol. 33, No. 6, pp. 63-69. (in Chinese).
- [6] Dharma, R.B. and Tan, K.H., "Rotational Capacity of Steel I-beams under Fire Conditions Part I: Experimental Study", *Engineering Structures*, 2007, Vol. 29, No. 9, pp. 2391-2402.
- [7] Tan, K.H., Toh, W.S., Huang, Z.F. and Phng, G.H., "Structural Responses of Restrained Steel Columns at Elevated Temperatures. Part 1: Experiments", *Engineering Structures*, 2007, Vol. 29, No. 8, pp. 1641-1652.
- [8] Han, L.H., Wang, W.H. and Yu, H.X., "Experimental Behaviour of Reinforced Concrete (RC) Beam to Concrete-filled Steel Tubular (CFST) Column Frames Subjected to ISO-834 Standard Fire", *Engineering Structures*, 2010, Vol. 32, No. 10, pp. 3130-3144.
- [9] Li, G.Q. and Guo, S.X., "Experiment on Restrained Steel Beams Subjected to Heating and Cooling", *Journal of Constructional Steel Research*, 2008, Vol. 64, No. 3, pp. 268-274.

- [10] Shao, Y.B., Li, T., Seng, T.L. and Chiew, S.P., “Hysteretic Behaviour of Square Tubular T-joint with Chord Reinforcement under Axial Cyclic Loading”, *Journal of Constructional Steel Research*, 2011, Vol. 67, No. 1, pp. 140-149.
- [11] Feng, R. and Young, B., “Tests of Concrete-filled Stainless Steel Tubular T-joints”, *Journal of Constructional Steel Research*, 2008, Vol. 64, No. 11, pp. 1283-1293.
- [12] Feng, R. and Young, B., “Experimental Investigation of Cold-formed Stainless Steel Tubular T-joints”, *Thin-Walled Structures*, 2008, Vol. 46, No. 10, pp. 1129-1142.
- [13] Lee, M.M.K., and Llewelyn-Parry, A., “Offshore Tubular T-joints Reinforced with Internal Plain Annular Ring Stiffeners”, *Journal of Structural Engineering, ASCE*, 2004, Vol. 130, No. 6, pp. 942-951.
- [14] Shao, Y.B., “Study on Reinforcing Methods for Welded Tubular Joints Structures”, *Journal of Yantai University (Natural science and engineering edition)*, 2009, Vol. 22, No. 4, pp. 312-320.
- [15] Liu, M.L., Zhao, J.C. and Yang, X.Y., “Study on Mechanical Performance of Tubular T-joints of Offshore Platform under Fire”, *The Ocean Engineering*, 2009, Vol. 27, No. 3, pp. 6-13. (in Chinese).
- [16] Liu, M.L., Zhao, J.C. and Jin, M., “Study on Load Capacity and Deformation of T-joints with Reinforced Ring at Elevated Temperatures”, *China Offshore Platform*, 2009, Vol. 24, No. 5, pp. 17-23. (in Chinese).
- [17] Nguyen, M.P., Fung, T.C. and Tan, K.H., “An Experimental Study of Structural Behaviours of CHS T-joints Subjected to Brace axial Compression in Fire Condition”, *Tubular Structures X III*, Hong Kong, 2010, pp. 725-732.
- [18] Nguyen, M.P., Tan, K.H. and Fung, T.C., “Numerical Models and Parametric Study on Ultimate Strength of CHS T-joints Subjected to Brace Axial Compression under Fire Condition”, *Tubular Structures X III*, Hong Kong, 2010, pp. 733-740.
- [19] Jin, M., Zhao, J.C., Chang, J. and Zhang, D.X., “Experimental Study and Parametric Study on the Post-fire Behavior of Tubular T-joint”, *Journal of Constructional Steel Research*, 2012, Vol. 70, pp. 93-100.
- [20] Yu, W.J., Zhao, J.C., Luo, H.X., Shi, J.Y. and Zhang, D.X., “Experimental Study on Mechanical Behavior of an Impacted Steel Tubular T-joint in Fire”, *Journal of Constructional Steel Research*, 2011, Vol. 67, No. 9, pp. 1376-1385.
- [21] Zhao, X.L., “Deformation Limit and Ultimate Strength of Welded T-joints in Cold-formed RHS Sections”, *Journal of Constructional Steel Research*, 2000, Vol. 53, No. 2, pp. 149-165.